Synthesis and Helical Structure of Poly(*N*-butynylamide)s Having Various Side Chains, Where the Helix Is Highly Affected by the Methyl Branch and the Lactone Moiety

Yuji Suzuki,[†] Junichi Tabei,[†] Masashi Shiotsuki,[†] Yoshihito Inai,[‡] Fumio Sanda,*[,†] and Toshio Masuda*[,†]

Department of Polymer Chemistry, Graduate School of Engineering, Kyoto University, Katsura Campus, Kyoto 615-8510, Japan, and Department of Environmental Technology and Urban Planning, Shikumi College, Graduate School of Engineering, Nagoya Institute of Technology, Gokiso-cho, Showa-ku, Nagoya 466-8555, Japan

Received October 18, 2007; Revised Manuscript Received December 2, 2007

ABSTRACT: *N*-Butynylamides, (*S*)-HC≡$CCH_2CH_2NHCOCH_2CH(CH_3)CH_2CH_3$ (**1**), (*R*)-HC≡CCH_2CH_2-$NHCOCH_2CH(CH_3)CH_2CH_2CH_2CH(CH_3)_2$ (**2**), (*S*)-HC≡$CCH_2CH_2NHCOCH(CH_3)CH_2CH_2CH_2CH_2CH_2CH_3$ (**3**), (1*S*)-HC≡$CCH_2CH_2NHCOC_9H_{13}O_2$ (**4**, $COC_9H_{13}O_2$ = camphanyl), and HC≡$CCH_2CH_2NHCOCH_2CH_2CH_2CH_2$-$CH_3$ (**5**) were polymerized with $[(nbd)RhCl]_2$-Et_3N in $CHCl_3$ to obtain *cis*-stereoregular poly(*N*-butynylamide)s [poly(**1**)−poly(**5**)]. CD and IR spectroscopic studies revealed that poly(**1**)−poly(**4**) having chiral substituents in the side chains took predominantly one-handed helical structure stabilized by intramolecular hydrogen bonds between the pendent amide groups in $CHCl_3$. The helical structure of poly(**1**)−poly(**3**) was more stable to heating than that of the corresponding poly(*N*-propargylamide)s reported so far. In contrast, poly(**4**) having bulky lactone moieties changed the helical tightness according to temperature. The helical structure of poly(**3**) having α-methyl branch was much more stable to MeOH addition than that of poly(**1**) and poly(**2**) having *β*-methyl branch. The persistence length of the poly(*N*-butynylamide)s was nearly the same as that of poly(*N*-propargylcarbamate)s, but shorter than that of poly(*N*-propargylamide)s. Simulation of CD spectra was carried out for helical forms of a poly(*N*-butynylamide) to specify the asymmetric conformations.

Introduction

Biomacromolecules such as DNA[1] and proteins[2] take one-handed helical structure caused by the homochirality of their components. Their biological activities are based on elegant and sophisticated higher order structures. Artificial helical polymers have been extensively synthesized by imitating naturally derived helices, dating back to the discovery of isotactic polypropylene by Natta and co-workers.[3] Nowadays, development of chiral catalysts and remarkable progress in synthetic technique enable the synthesis of various helical polymers such as poly(alkyl methacrylate)s,[4] polychloral,[5] polyisocyanides,[6] polyisocyanates,[7] and polysilanes.[8] These synthetic helical polymers attract interest due to their potential of practical applications including molecular recognition materials, chiral catalysts, ferroelectric liquid crystals, and chemical sensors.[4c,6c,9]

Substituted polyacetylenes take a helical conformation, when the geometric structure of the main chain has a sufficient regularity. The polymerization of monosubstituted acetylenes with rhodium catalysts affords *cis*-stereoregular polyacetylenes,[10] some of which take a helical structure with predominantly one-handed screw sense by introducing chiral substituents[11] into the side chain or by interacting with chiral compounds.[12] We have reported that rhodium-based *cis*-stereoregular poly(*N*-propargylamide)s form a helical structure, which is stabilized by intramolecular hydrogen bonds along with steric repulsion between the side chains, the biomimetically same way as peptides and proteins.[13] Poly(*N*-propargylamide)s change the conformation by external stimuli such as heat and the addition of polar solvents, which disturb the formation of intramolecular hydrogen bonds stabilizing the helical structure. In the course of our study on helical poly(*N*-propargylamide)s, we have examined the effect of the distance between the main chain and amide group on the secondary structure, and we found that a poly(*N*-butynylamide) having two methylenes between the main chain and amide group also constructs a helical structure stabilized by a way similar to that of poly(*N*-propargylamide)s.[13a] Upon synthesizing a series of poly(*N*-propargylamide)s, we have found a remarkable substituent effect on the helix formation and stability, while the substituent effect of poly(*N*-butynylamide)s have not been examined yet. The present study deals with the synthesis of novel poly(*N*-butynylamide)s having various side chains (Scheme 1) and determination of the effect of the methyl branch and lactone on the helical conformation of the polymers, together with the solvent effect on the helix and relative persistence length. It also compares the helical structures and ways of intramolecular hydrogen bonds between poly(*N*-butynylamide)s and poly(*N*-propargylamide)s by the

Scheme 1

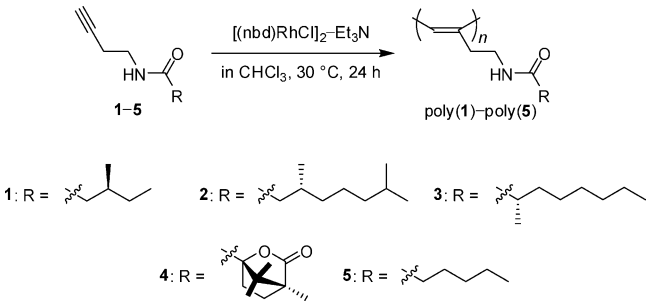

* To whom all correspondence should be addressed. E-mail: (F.S.) sanda@adv.polym.kyoto-u.ac.jp; (T.M.) masuda@adv.polym.kyoto-u.ac.jp.
[†] Kyoto University.
[‡] Nagoya Institute of Technology.

10.1021/ma702316f CCC: $40.75
Published on Web 01/09/2008

Table 1. Polymerization of 1−5[a]

monomer	yield[b] (%)	M_n[d]	M_w/M_n[d]	$[\alpha]_D$[e] (deg)
1	54[c]	10 200	1.48	+306
2	26	10 900	2.17	−499
3	43	9100	2.56	+355
4	42	22 000	1.58	+609
5	46	16 000	1.79	0

[a] Polymerized with [(nbd)RhCl]$_2$-Et_3N in $CHCl_3$ at 30 °C for 24 h. $[M]_0$ = 1.0 M, $[M]_0$/[Rh] = 100, $[Et_3N]$/[Rh] = 2. [b] MeOH-insoluble part. [c] Et_2O-insoluble part. [d] Estimated by GPC ($CHCl_3$, PSt standard). [e] Measured in $CHCl_3$ (c = 0.01−0.10 g/dL).

conformational analysis and CD simulation based on the molecular orbital method.

Experimental Section

Measurements. Melting points (mp) were measured with a Yanako micromelting point apparatus. Specific rotations ($[\alpha]_D$) and IR spectra were measured with a JASCO DIP-1000 digital polarimeter and a FTIR-4100 spectrophotometer, respectively. NMR (^{1}H, 400 MHz; ^{13}C, 100 MHz) spectra were recorded on a JEOL EX-400 spectrometer. Elemental analyses were conducted at the Microanalytical Center of Kyoto University. X-ray crystallographic analysis was carried out on a Rigaku AFC5R diffractometer. Number-average molecular weights (M_n) and molecular weight distributions (M_w/M_n) of polymers were estimated by GPC (Shodex columns K803, K804, K805) eluted with $CHCl_3$ calibrated by polystyrene standards. CD and UV−vis spectra were recorded on a JASCO J-820 spectropolarimeter.

Materials. (*S*)-(+)-2-Methyloctanoic acid (Japan Energy), (1*S*)-(−)-camphanic acid (Aldrich), hexanoic acid (Wako), and 4-(4,6-dimethoxy-1,3,5-triazin-2-yl)-4-methylmorpholinium chloride (Tokuyama) were used as received. Toluene-4-sulfonic acid 3-butynyl ester,[14] (*S*)-3-methylpentanoic acid,[13a] and (*R*)-3,7-dimethyloctanoic acid[13e] were prepared according to the literature. $CHCl_3$ used for polymerization was distilled prior to use.

Synthesis of Monomers 1−5. Monomer **1** was synthesized as follows. Liquid ammonia (200 mL) was introduced into an autoclave that was cooled to −78 °C, then toluene-4-sulfonic acid 3-butynyl ester (10.7 g, 47 mmol) was added, and the autoclave was closed. The resulting mixture was stirred at room temperature for 24 h, and the autoclave was opened to allow residual ammonia to evaporate. Et_2O was added to the residue, and the mixture was filtered. The filtrate was distilled under reduced pressure (100 °C/120 mmHg) to obtain 3-butynylamine as colorless liquid in 29% yield. ^{1}H NMR ($CDCl_3$): δ 1.72 (NH_2, br, 2H), 2.03 (C≡CH, s, 1H), 2.33 (C≡CCH_2, t, J = 6.3 Hz, 2H), 2.85 (CH_2NH_2, t, J = 6.4 Hz, 2H). ^{13}C NMR ($CDCl_3$): δ 23.28, 40.71, 69.63, 82.26. 4-(4,6-Dimethoxy-1,3,5-triazin-2-yl)-4-methylmorpholinium chloride[15] (1.67 g, 6 mmol) was added to a solution of 3-butynylamine (0.41 g, 6 mmol) and (*S*)-3-methylpentanoic acid (0.70 g, 6 mmol) in THF (100 mL), and the resulting mixture was stirred at room temperature overnight. It was concentrated on a rotary evaporator. Et_2O was added to the residue, and the resulting solution was washed with 2 M HCl and saturated aqueous $NaHCO_3$, dried over anhydrous $MgSO_4$, and concentrated. Monomer **1** was isolated by column chromatography on silica gel eluted with hexane/ethyl acetate = 1/1 (v/v). Yield 0.43 g (2.6 mmol, 43%). Monomers **2**−**5** were prepared in a similar way. **1**: $[\alpha]_D$ = +5.8 deg (c = 0.27 g/dL in $CHCl_3$). ^{1}H NMR ($CDCl_3$): δ 0.88−0.90 (CH$_2$CH_3, m, 3H), 0.92 (CHCH_3, d, J = 6.0 Hz, 3H), 1.21−1.23 (CHHCH$_3$, m, 1H), 1.37−1.39 (CHHCH$_3$, m, 1H), 1.90−1.91 (CH, m, 1H), 1.96−1.98 (COCHH, m, 1H), 2.00 (C≡CH, s, 1H), 2.19−2.22 (COCHH, m, 1H), 2.41 (C≡CCH_2, br, 2H), 3.41 (CH_2NH, br, 2H), 5.97 (NH, br, 1H). ^{13}C NMR ($CDCl_3$): δ 11.25, 19.09, 19.41, 29.34, 32.27, 37.84, 44.07, 69.89, 81.59, 172.7. IR (in $CHCl_3$): 3451, 2964, 1663, 1517, 1462, 1264, 913, 775 cm^{-1}. Anal. Calcd for $C_{10}H_{17}NO$: C, 71.81; H, 10.25; N, 8.37. Found: C, 71.60; H, 10.31; N, 8.31. **2**: yield 56%, mp 45.0−46.0 °C; $[\alpha]_D$ = +5.1 deg (c = 0.11 g/dL in $CHCl_3$). ^{1}H NMR ($CDCl_3$): δ 0.84 (CH(CH_3)$_2$, d, J = 6.8 Hz, 6H), 0.91 (CHCH_3, d, J = 6.0 Hz, 3H), 1.13−1.14 (CH_2i-Pr, m, 2H), 1.15−1.16 (C*HCH_2CH$_2$, m, 2H), 1.27−1.30 (CH_2i-Bu, m, 2H), 1.50−1.54 [CH(CH$_3$)$_2$, m, 1H], 1.90−1.91 (COCHH, m, 1H), 1.94−1.96 (COCHH, m, 1H), 1.98 (C≡CH, s, 1H), 2.17−2.20 (C*H, m, 1H), 2.41 (C≡CCH_2, t, J = 6.3 Hz, 2H), 3.39−3.44 (CH_2-NH, m, 2H), 5.76 (NH, br, 1H). ^{13}C NMR ($CDCl_3$): δ 19.54, 19.67, 22.69, 24.71, 27.95, 30.83, 37.07, 37.86, 39.08, 44.64, 69.91, 81.66, 172.6. IR (in $CHCl_3$): 2958, 1664, 1515, 1217, 1016, 780, 759 cm^{-1}. Anal. Calcd for $C_{14}H_{25}NO$: C, 73.90; H, 11.11; N, 6.77. Found: C, 73.20; H, 10.93; N, 6.85. **3**: yield 45%, mp 47.0−49.0 °C; $[\alpha]_D$ = +5.8 deg (c = 0.10 g/dL in $CHCl_3$). ^{1}H NMR ($CDCl_3$): δ 0.87 (CH$_2$CH_3, t, J = 7.0 Hz, 3H), 1.14 (CHCH_3, d, J = 6.8 Hz, 3H), 1.27[(CH_2)$_4$CH$_3$, br, 8H], 1.37−1.40 (C*HCHH, m, 1H), 1.63−1.64 (CH*CHH, m, 1H), 2.00 (C≡CH, s, 1H), 2.16−2.21 (CH, m, 1H), 2.41 (C≡CCH_2, t, J = 6.4 Hz, 2H), 3.38−3.44 (CH_2NH, m, 2H), 5.81 (NH, br, 1H). ^{13}C NMR ($CDCl_3$): δ 14.06, 17.85, 19.51, 22.62, 27.43, 29.29, 31.74, 34.38, 37.72, 41.62, 69.78, 81.62, 176.6. IR (in $CHCl_3$): 3450, 2930, 1665, 1515, 1220, 782, 772, 685 cm^{-1}. Anal. Calcd for $C_{13}H_{23}NO$: C, 74.59; H, 11.07; N, 6.69. Found: C, 74.34; H, 10.99; N, 6.67. **4**: yield 43%, mp 93.5−95.5 °C; $[\alpha]_D$ = −7.6 deg (c = 0.11 g/dL in $CHCl_3$). ^{1}H NMR ($CDCl_3$): δ 0.93 (CCH_3, s, 3H), 1.12 [C(CH_3)$_2$, s, 6H], 1.67−1.70 (CHH, m, 1H), 1.89−1.91 (CHH, m, 1H), 1.97−1.98 (COCCHH, m, 1H), 2.02 (C≡CH, s, 1H), 2.44 (C≡CCH_2, br, 2H), 2.52−2.54 (COCCHH, m, 1H), 3.37−3.42 (CHHNH, m, 1H), 3.52−3.57 (CHHNH, m, 1H), 6.80 (NH, br, 1H). ^{13}C NMR ($CDCl_3$): δ 9.59, 16.49, 16.60, 19.32, 28.96, 30.16, 37.61, 53.78, 55.19, 70.15, 80.89,

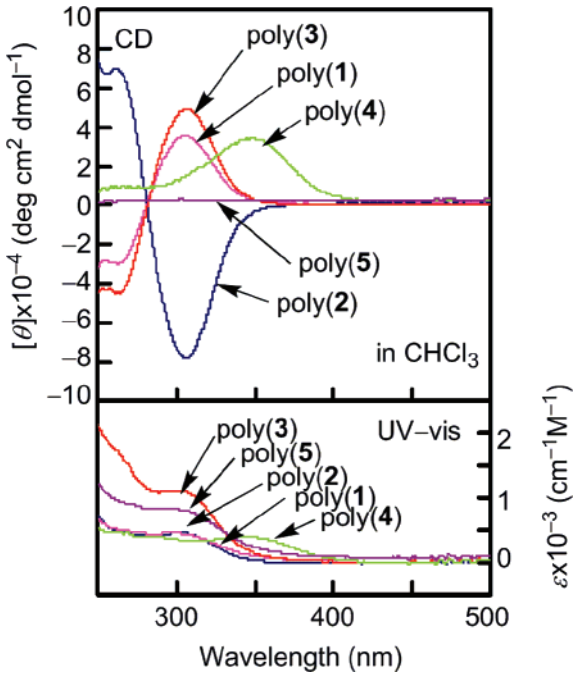

Figure 1. CD and UV−vis spectra of poly(**1**)−poly(**5**) measured in $CHCl_3$ (c = 0.07−0.46 mM) at 20 °C.

Table 2. Solution State IR Absorption of Amide and Ester Groups of 1−5 and Poly(1)−Poly(5)[a]

	wavenumber (cm^{-1})		
compound	C=O of amide	N−H of amide	C=O of ester
1	1663	1517	
poly(**1**)	1629	1548	
2	1664	1515	
poly(**2**)	1630	1550	
3	1665	1513	
poly(**3**)	1631	1548	
4	1677	1533	1785
poly(**4**)	1655	1541	1776
5	1667	1520	
poly(**5**)	1628	1554	

[a] Measured in $CHCl_3$ (c = 1−50 mM) at room temperature.

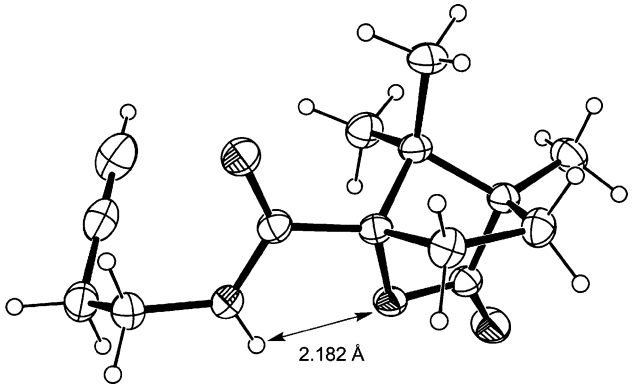

Figure 2. ORTEP drawing of **4**.

92.39, 167.0, 178.2. IR (in $CHCl_3$): 3432, 3308, 3019, 1785, 1677, 1533, 1217, 1168, 1123, 924, 778, 669 cm^{-1}. Anal. Calcd for $C_{14}H_{19}NO_3$: C, 67.13; H, 7.58; N, 5.51. Found: C, 66.96; H, 7.54; N, 5.47. **5**: yield 51%, mp 45.0−46.5 °C. ^1H NMR ($CDCl_3$): δ 0.86 (CH_3, t, J = 6.8 Hz, 3H), 1.29−1.33 ($CH_2CH_2CH_3$, m, 4H), 1.62−1.64 ($COCH_2CH_2$, m, 2H), 2.01 (C≡C*H*, s, 1H), 2.17−2.21 ($COCH_2$, m, 2H), 2.38 (C≡CCH_2, t, J = 6.3 Hz, 2H), 3.39−3.42 (CH_2NH, m, 2H), 5.84 (N*H*, br, 1H). ^{13}C NMR ($CDCl_3$): δ 13.93, 19.48, 22.31, 25.39, 31.40, 36.73, 37.89, 69.92, 81.59, 173.3. IR (in $CHCl_3$): 3013, 2360, 1667, 1520, 1472, 1368, 1203, 820, 755 cm^{-1}. Anal. Calcd for $C_{10}H_{17}NO$: C, 71.81; H, 10.25; N, 8.37. Found: C, 71.55; H, 10.34; N, 8.29.

Polymerization. A solution of $[(nbd)RhCl]_2$ (2.3 mg, 5.0 μmol) and Et_3N (1.0 mg, 10.0 μmol) in distilled $CHCl_3$ (0.25 mL) was added to a solution of a monomer (0.5 mmol) in distilled $CHCl_3$ (0.25 mL) under nitrogen, and the resulting solution was kept at 30 °C for 24 h. The reaction mixture was poured into Et_2O or MeOH to precipitate a polymer. It was separated by filtration and dried under reduced pressure.

Spectroscopic Data of the Polymers. Poly(1). ^1H NMR ($CDCl_3$): δ 0.7−1.1 (CH_2CH_3, $CHCH_3$, br, 6H), 1.1−1.3 ($CHHCH_3$, br, 1H), 1.3−1.4 ($CHHCH_3$, br, 1H), 1.8−2.1 (C*H*, $COCH_2$, br, 3H), 2.1−2.8 (C=CCH_2, br, 2H), 3.0−3.6 (CH_2NH, br, 2H), 5.6−6.3 (C=C*H*, br, 1H), 8.2−9.1 (N*H*, br, 1H). IR (in $CHCl_3$): 3621, 2974, 2359, 1629, 1548, 1218, 1046, 782, 669 cm^{-1}. **Poly(2).** ^1H NMR ($CDCl_3$): δ 0.7−1.0 ($CH(CH_3)_2$, $CHCH_3$, br, 9H), 1.0−1.2 (CH_2i-Pr, C*HCH$_2$CH$_2$, br, 4H), 1.2−1.4 (CH_2i-Bu, br, 2H), 1.4−1.6 [$CH(CH_3)_2$, br, 1H], 1.8−2.2 ($COCH_2$, br, 2H), 2.2−2.6 (C*H*, C=CCH_2, br, 3H), 3.0−3.9 (CH_2NH, br, 2H), 5.7−6.3(C=C*H*, br, 1H), 8.5−9.0 (N*H*, br, 1H). IR (in $CHCl_3$): 3622, 2962, 1630, 1550, 1451, 1383, 1214, 1016, 812, 762 cm^{-1}. **Poly(3).** ^1H NMR ($CDCl_3$): δ 0.7−1.0 (CH_2CH_3, br, 3H), 1.0−1.2 ($CHCH_3$, br, 3H), 1.2−1.5 [$(CH_2)_4CH_3$, C*HCH*H*, br, 9H], 1.5−1.8 (C*HCH*H*, br, 1H), 2.0−2.8 (C*H*, C=CCH_2, br, 3H), 3.0−3.9 (CH_2NH, br, 2H), 5.6−6.3 (C=C*H*, br, 1H), 8.4−9.1 (N*H*, br, 1H). IR (in $CHCl_3$): 3279, 2929, 2856, 1631, 1549, 1452, 1225, 1215, 783, 688 cm^{-1}. **Poly(4).** ^1H NMR ($CDCl_3$): δ 0.8−1.0 (CCH_3, br, 1H), 1.0−1.2 [$C(CH_3)_2$, br, 6H], 1.5−1.8 (C*H*H, br, 1H), 1.8−2.1 (CH*H*, COCC*H*H, br, 2H), 2.4−2.7 (C=CCH_2, COCCH*H*, br, 3H), 3.2−3.6 (CH_2NH, br, 2H), 5.9−6.2 (C=C*H*, br, 1H), 7.5−7.9 (N*H*, br, 1H). IR (in $CHCl_3$): 3627, 3359, 2975, 2343, 1776, 1655, 1541, 1447, 1049, 917, 826, 691 cm^{-1}. **Poly(5).** ^1H NMR ($CDCl_3$): δ 0.7−1.0 (CH_3, br, 3H), 1.2−1.4 (CH_2CH_3, br, 2H), 1.4−1.5 (CH_2-Et, br, 2H), 1.5−1.7 (CH_2Pr, br, 2H), 2.0−2.6 ($COCH_2$, C=CCH_2, br, 4H), 2.9−3.6 (CH_2NH, br, 2H), 5.6−6.2 (C=C*H*, br, 1H), 8.4−9.0 (N*H*, br, 1H). IR (in $CHCl_3$): 3281, 2931, 2361, 1628, 1554, 1223, 1215, 794, 778 cm^{-1}.

Computation of Simulated CD Spectra. Theoretical CD spectra were predicted for a 18-mer of *N*-butynylacetamide (R = CH_3 in Scheme 1). Energy minimization was carried out with molecular mechanics (MM) based on the MMFF94 force field[16] in Wavefunction, Spartan '04 Windows. Helical conformers obtained were subjected to CD simulation based on the time-dependent SCF (ZINDO/S) method.[17] Electronic transition and chiroptical parameters were computed on Gaussian 03 basically according to refs 17 and 18. The low-energy transition states of 200 were predicted under the condition of a CI number of 200 × 200, including each oscillator strength (f_{vel}) and rotatory strength (R_{vel}) in velocity form. Theoretical CD spectra were produced by using the R_{vel}-wavelength data with a wavelength-based Gaussian function of 10 nm tentatively used for a half of 1/e-bandwidth.[17a,d,e,19] The corresponding absorption profiles were also predicted using the f_{vel}-wavelength data with a similar Gaussian function.[19]

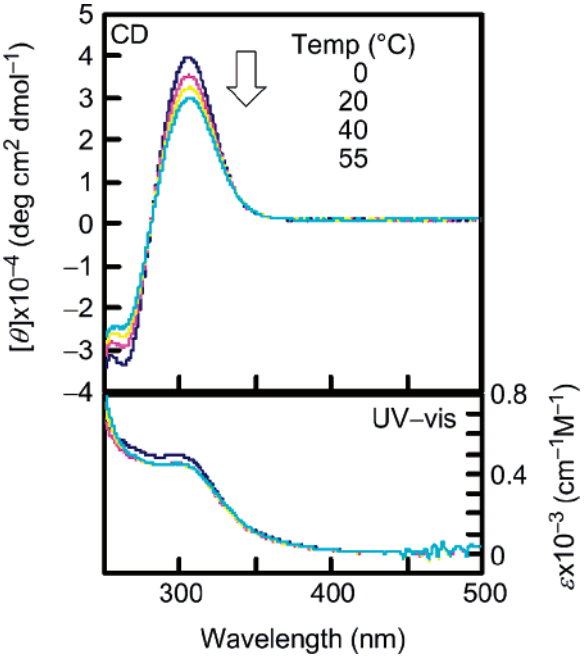

Figure 3. CD and UV−vis spectra of poly(**1**) measured in $CHCl_3$ (c = 0.23 mM) at various temperatures.

Results and Discussion

Polymerization. The polymerization of monosubstituted acetylenes using a rhodium catalyst affords corresponding *cis*-stereoregular polymers[10] even though monomers have polar functional groups such as amide and ester.[20] Thus, the polymerization of *N*-butynylamides **1**−**5** was conducted with $[(nbd)RhCl]_2$−Et_3N as a catalyst in $CHCl_3$ to give the polymers [poly(**1**)−poly(**5**)] with moderate molecular weights (M_n = 9100−22 000) in 26−54% yields as listed in Table 1. The relatively lower polymer yields than those of poly(*N*-propargylamide)s[13f] may be due to the lower electron density of the ethynyl group, which is unfavorable to coordination with the rhodium catalyst. In fact, the average atomic charge of the ethynyl carbon atoms of **1** was −0.188, while that of *N*-propargyl 3-methylpentanamide was −0.198.[21] The resulting polymers showed a ^1H NMR signal assignable to the *cis*-olefinic proton in the main chain around 6 ppm, and the integration ratio of the signal confirmed that the *cis* content of the polymers was quantitative in every case. The IR spectroscopic data of the polymers also supported the formation of poly(*N*-butynylamide)s. All the polymers were soluble in $CHCl_3$, and chiral polymers [poly(**1**)−poly(**4**)] exhibited large optical rotations (|[α]| = 306−609°) in the solvent compared to those of the monomers (|[α]| = 5.1−7.6°).

Secondary Structure. Figure 1 depicts the CD and UV−vis spectra of poly(**1**)−poly(**5**) measured in $CHCl_3$ at 20 °C. Poly(**1**)−poly(**3**), having chiral alkyl side chains, exhibited intense Cotton effects around 300 nm, and poly(**4**), having a chiral lactone, did the same around 340 nm. They exhibited UV−vis absorption at the same regions as the CD spectra, which

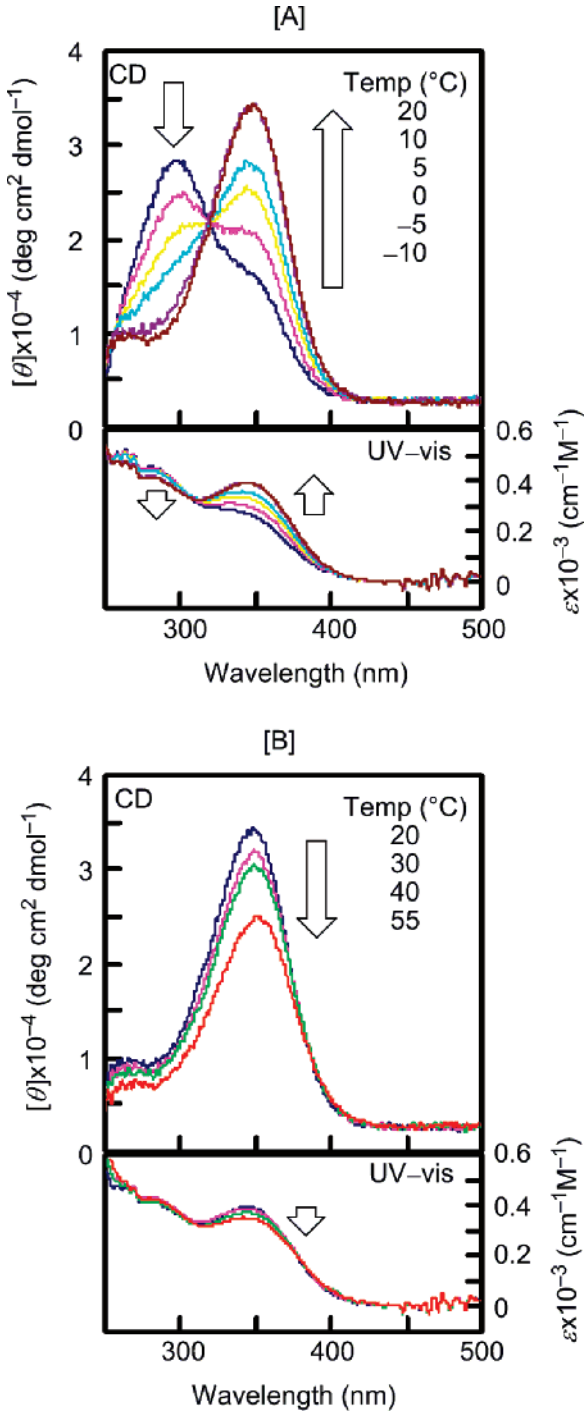

Figure 4. CD and UV−vis spectra of poly(**4**) measured in $CHCl_3$ (c = 0.36 mM) at [A] −10−20 °C and [B] 20−55 °C.

confirmed that the chiroptical property was based on the conjugated polyacetylene main chain chromophore. Hence, it is concluded that poly(**1**)−poly(**4**) take helical structures with predominantly one-handed screw sense in $CHCl_3$. On the other hand, poly(**5**) having achiral side chain exhibited no Cotton effect. The shape of Cotton effects of poly(**1**)−poly(**3**) is different from that of common poly(*N*-propargylamide)s[13] but similar to that of poly(*N*-propargylcarbamate)s[22] reported so far. Namely, most of poly(*N*-propargylamide)s[13] show a Cotton effect around 390 nm, whereas poly(**1**)−poly(**3**) do it around 300 nm, which indicates that the helix of these three polymers is tighter than that of poly(*N*-propargylamide)s, leading to a shorter conjugation length.[23] Poly(**1**) and poly(**3**) possessing (*S*)-configuration in the chiral side chains exhibited specific rotations and Cotton effects with the same sign, which indicates that the polymers have the same helical screw sense each other. This result contrasts to the observation of odd−even rules in chiroptical properties of several chiral polymers such as polysilanes,[24a] polythiophenes,[24b] and polyisocyanides;[24c] for example, the helical sense of polythiophenes having identical chiral units alternates upon sequential variation of the spacer length. Such effect is not observed in the present polymers exceptionally as in the case of poly(*N*-propargylamide)s[13a] and poly(propiolic ester)s.[11e] The position of chiral center does not affect the tightness of helical structure of the polymers in the present study.

Confirmation of Hydrogen Bonding. It is likely that the helical structures of poly(**1**)−poly(**4**) are stabilized by intramolecular hydrogen bonds between the pendent amide groups in $CHCl_3$. In order to confirm this, the IR spectra of the monomers and polymers were measured in $CHCl_3$ (c = 1−50 mM) as summarized in Table 2. The amide I and II absorption peaks of monomers **1**−**5** were observed at 1663−1677 and 1513−1533 cm^{-1}, while those of poly(**1**)−poly(**5**) were observed at 8−39 cm^{-1} lower and higher wavenumbers, respectively, irrespective of the concentration. These results clearly indicate that intramolecular hydrogen bonds are formed between the amide groups of the polymers. We have previously reported that poly(3-butynyl ester)s, ester analogues of poly(*N*-butynylamide)s, do not form a helical structure, presumably due to the absence of hydrogen bonding.[13a] Consequently, it is considered that the helical structure of poly(*N*-butynylamide)s is stabilized by intramolecular hydrogen bonds between the pendent amide groups. It can be considered that intermolecular hydrogen bonding does not form because of the low concentration of the polymer solutions.

The carbonyl absorption of ester group of poly(**4**) also shifted by 9 cm^{-1} from that of **4** as listed in Table 2. It should be noted that the shifts of the amide I and II absorption peaks from **4** to poly(**4**) (22 and 8 cm^{-1}) were smaller than those from the other monomers to the corresponding polymers (31−39 cm^{-1}). This fact indicates that the ester group of lactone of poly(**4**) participates in hydrogen bonds between the amide groups. In order to obtain information on the intramolecular hydrogen bonding involving the lactone in side chains, we analyzed the conformation of **4** by X-ray crystallography. As shown in Figure 2, the interatomic distance between the amide hydrogen and ether oxygen was 2.182 Å. It is concluded that these two atoms form a hydrogen bond, which supports the assumption that the lactone moieties participate in the intramolecular hydrogen bonds between the amide groups of poly(**4**). This result presumably relates to the different helicity of poly(**4**) from that of poly(**1**)−poly(**3**).

Effect of Temperature on Helical Conformation. Figure 3 depicts the CD and UV−vis spectra of poly(**1**) measured in $CHCl_3$ at various temperatures. By raising temperature, the intensity of Cotton effect was slightly decreased, and obvious Cotton effect remained even at 55 °C as reported so far.[13a] Poly(**2**) and poly(**3**) showed a similar tendency; thus the helical conformation of poly(**1**)−poly(**3**) was quite stable upon heating. The helical conformation of these polymers was thermally more stable than that of the corresponding poly(*N*-propargylamide)s reported so far;[13] at 55 °C, poly(**1**) decreased the intensity of Cotton effect to 75% of that at 0 °C, while the corresponding poly(*N*-propargylamide) decreased it to 30%. On the other hand, poly(**4**) showed a completely dissimilar tendency to poly(**1**)−poly(**3**) upon heating. When the temperature was raised from −10 to +20 °C, the intensity of the peak at 280 nm was

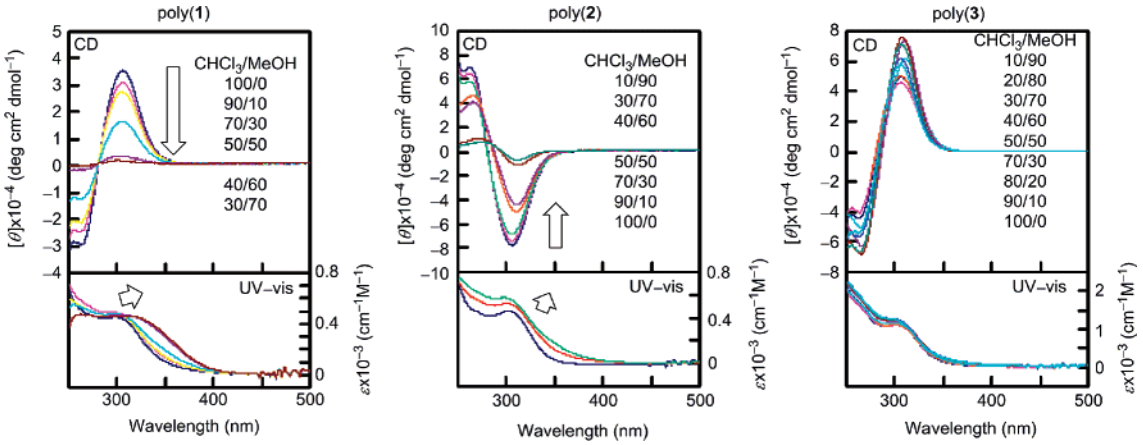

Figure 5. CD and UV−vis spectra of poly(**1**)−poly(**3**) measured in $CHCl_3$/MeOH (c = 0.18−0.46 mM) at 20 °C.

decreased and the intensity of the peak at 340 nm was increased in both CD and UV−vis spectra as depicted in Figure 4A, indicating that the helix of poly(**4**) became loose upon heating at this temperature region.[23] The intensity of the peak at 340 nm in the CD and UV−vis spectra was decreased by further raising temperature above 20 °C (Figure 4B), presumably due to partial transformation from helical conformation into random one upon heating. The thermal responsiveness of the chiroptical properties was reversible in the whole temperature range.

Effect of MeOH Addition on Helical Conformation. As described in the discussion on the solution state IR spectroscopy, it is likely that the helical structure of poly(*N*-butynylamide)s is stabilized by intramolecular hydrogen bonds. We examined the effect of MeOH addition, which should disturb the formation of hydrogen bonds. Figure 5 depicts the CD and UV−vis spectra of poly(**1**)−poly(**3**) measured in $CHCl_3$/MeOH at 20 °C. Poly(**1**) and poly(**2**) decreased the intensity of Cotton effect upon raising the MeOH content; the Cotton effect almost disappeared when the MeOH content became 60−90%. The CD spectral change is attributable to the deformation from helical state into random. On the other hand, poly(**3**) did not decrease the Cotton effect so much, even when the MeOH content became 90%. The position of methyl branch dramatically affected the helix stability of the polymers. It is considered that the methyl branch near the amide group can shield the hydrogen bonds from MeOH, resulting in the stabilization of the helical structure. The helix of poly(**3**) is much more stable than that of the poly(*N*-propargylamide) counterpart.[13e]

Persistence Length of the Helical Domain. The persistence length of the helical domain was investigated by the chiral/achiral copolymerization of **2** with **5** to estimate the helix stability. As shown in Figure 6A, the $[\alpha]_D$ and $[\theta]_{max}$ of the copolymers were decreased upon raising the chiral content, and an apparent chiral amplification was observed. In addition, the polymers of **1** with various monomer unit ratios of (*R*)- and (*S*)-forms also exhibited similar behavior as shown in Figure 6B.[25] These results demonstrate that the poly(*N*-butynylamide)s in the present study have a persistence length long enough to exhibit such a chiral amplification. The present poly(*N*-butynylamide)s seem to have almost the same persistence length as poly(*N*-propargylcarbamate)s,[22b] but a shorter one than that of poly(*N*-propargylamide)s[13e] judging from the degree of the chiral amplification. Thus, poly(*N*-butynylamide)s possess a higher population of the helix reversal point than poly(*N*-propargylamide)s. It should be noted that the helical structure of poly(**1**) is thermally more stable in spite of the shorter persistence length than that of poly(*N*-propargylamide)s. This

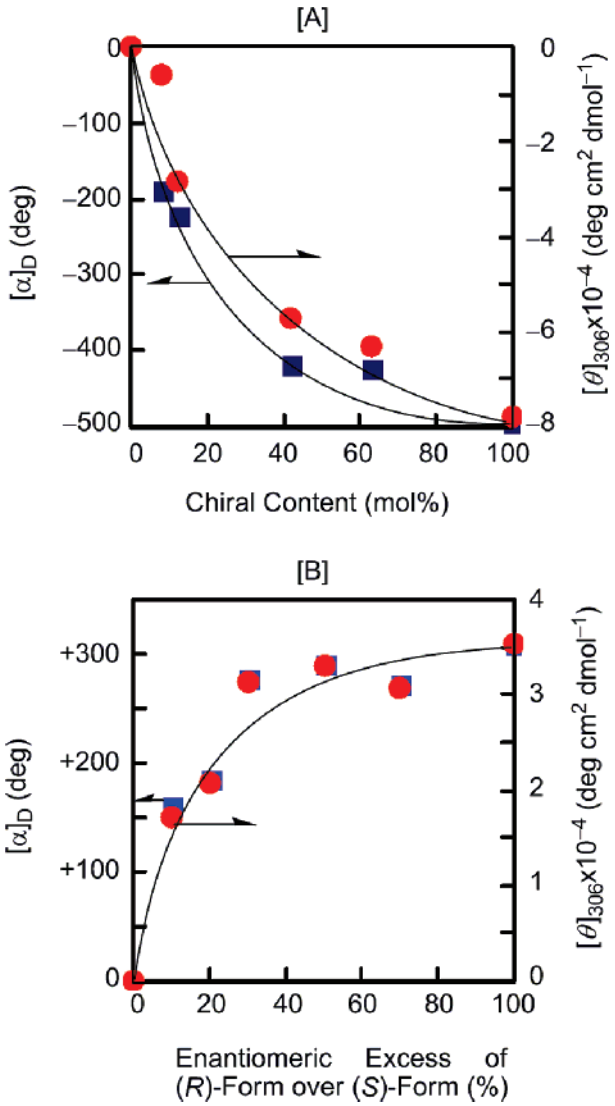

Figure 6. Plots of the optical rotation ($[\alpha]_D$) and CD intensity at the absorption maximum ($[\theta]_{max}$) [A] vs chiral content of poly(**2**-*co*-**5**), [B] vs enantiomeric excess of the monomer units in the copolymer of **1** [(*R*)-form] and the enantiomer [(*S*)-form].

is presumably caused by the tightly twisted structure of poly(**1**) compared to that of poly(*N*-propargylamide)s, which will be described in the following section.

Simulation of CD Spectra. To gain more structural information, theoretical computation of CD spectra was carried out for a 18-mer of *N*-butynylacetamide (R = CH_3 in Scheme 1). The

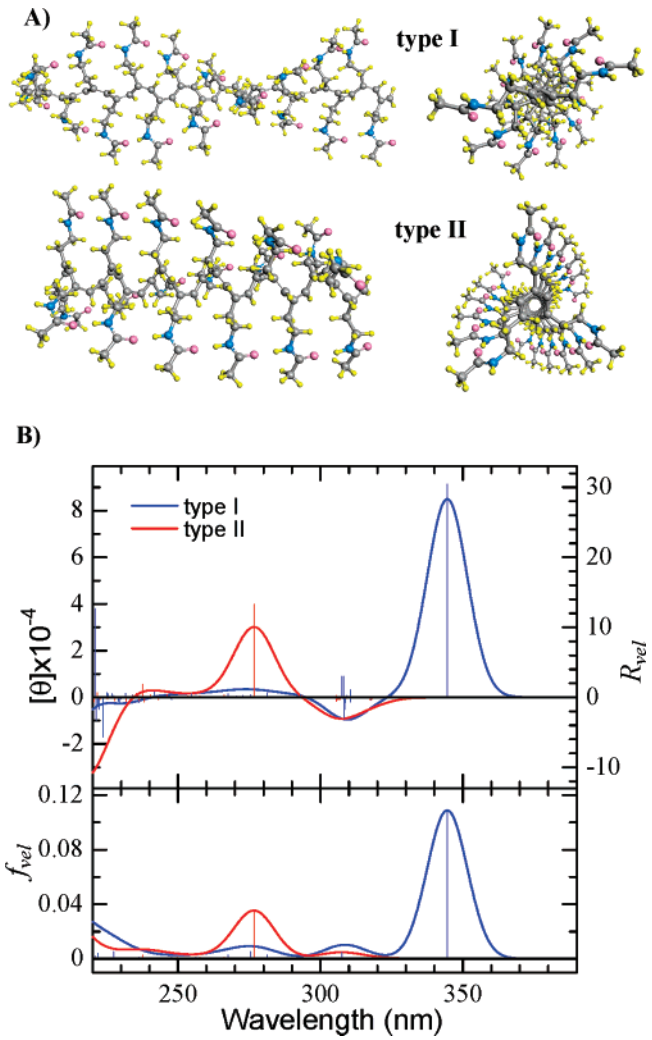

Figure 7. (A) Types I and II (*P*) helical conformations of a 18-mer of *N*-butynylacetamide. (B) Their simulated CD spectra and absorption profiles: $[\theta]$, R_{vel}, and f_{vel} of the polymer molecule are divided by 18 as the values per monomer unit.

MM calculation offered two helical conformers (types I and II: Figure 7A[26]) characterized by different dihedral angle (τ) at the single bond along the main chain: τ = ca. 130° (type I) and ca. 70° (type II). Type I takes a relatively extended helical backbone, while type II adopts a tightly twisted helical form. Type I forms intramolecular hydrogen bonding between *n*th and $(n + 2)$th units, and type II does it between *n*th and $(n + 3)$th units. Figure 7A corresponds to a right-handed (*P*) helix.[27] This achiral side chain will promise the same energy as the enantiomeric left-handed (*M*) helix.[27]

CD spectra of the two conformers as well as their absorption profiles (Figure 7B) largely differ from each other. Type I yields positive CD signals for a strong absorption band around 345 nm. In contrast, a prominent absorption band around 277 nm appears in type II. Such a blue shift should be attributed to a reduced degree of π-conjugation in the type II backbone due to its more perpendicular conformation. In addition, the CD spectrum of type II shows negative signals around 277 nm and positive ones at longer wavelengths. Consequently, the sign inversion of CD signals (apparently "split type") occurs in type II, although type I emphasizes a CD band with one sign.

A visual comparison between the experimental and simulated CD/absorption patterns allows us to estimate a preferential conformation of poly(**1**)−poly(**5**). Poly(**4**) shows positive CD signals for an absorption band around 350 nm, thus suggesting

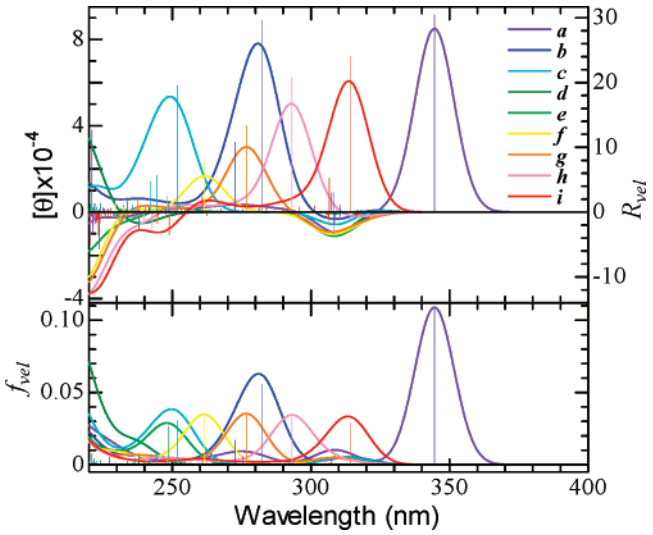

Figure 8. Simulated CD spectra and absorption profiles of a 18-mer of *N*-butynylacetamide in several helical conformations. The τ angles for the helical backbones are about 130° (***a***), 120° (***b***), 110° (***c***), 100° (***d***), 90° (***e***), 80° (***f***), 70° (***g***), 60° (***h***), and 50° (***i***). Curves ***a*** and ***g*** correspond to types I and II in Figure 7B, respectively. Each vertical scale is divided by 18 likewise in Figure 7B.

the occurrence of a type I (*P*) helical conformation. Poly(**1**)−poly(**3**) display an absorption band around 310 nm followed by a larger absorption band at shorter wavelengths. The corresponding CD spectra are characterized by two Cotton effects with the opposite sign. These spectral features suggest that poly(**2**) adopts a type II (*P*) helix, and that poly(**1**) and poly(**3**) with the opposite CD signs form a type II (*M*) helix. The optically inactive poly(**5**) displays an absorption profile to those of poly(**1**)−poly(**3**), thus implying the preference for a type II helix.

Main-chain torsion in the present polymer will largely influence its electronic transition states, likewise in the case of other conjugated molecular frames.[28] In addition, the backbone conformation in solution should thermally fluctuate more or less.[29] These circumstances might prevent us from specifying the dynamic conformations by using such spectroscopic data. Correspondingly, the relationship between the main-chain torsion and spectral pattern has been estimated to clarify these problems.

Figure 8 displays CD spectra simulated for several helices with various τ angles. CD spectra as well as absorption patterns are largely influenced by the main-chain conformation governing the degree of π-conjugation. Among the conformers of $\tau \sim 50$−130°, the absorption position at longer wavelengths of type I ($\tau \sim 130°$) is the closest to that of poly(**4**). A "split-like" CD pattern around 275−310 nm of $\tau \sim 70°$ (type I) or around 260−310 nm of $\tau \sim 80°$ reproduces the experimental CD of poly(**1**)−poly(**3**) well. In contrast, the other conformers do not produce such a split-like CD pattern around 260−310 nm. Therefore, the structural discussion described in Figure 7 should be essentially valid even if the influence of conformational fluctuations on the electronic spectra is taken into account.

Conclusion

In the present study, we have demonstrated the polymerization of *N*-butynylamides **1**−**5** having various substituents using a rhodium catalyst to obtain the polymers with moderate molecular weights and almost quantitative *cis* content of the main chain. They took helical structures with predominantly one-handed

screw sense that were stabilized by intramolecular hydrogen bonds between the pendent amide groups in a manner similar to that of poly(*N*-propargylamide)s. The helical structure of poly(*N*-butynylamide)s was more stable upon heating and addition of MeOH than that of poly(*N*-propargylamide)s in spite of the shorter helix persistence length. The helical tightness and number of hydrogen-bonding strands possibly explain the reason for the difference between the two series of polymers. Namely, poly(*N*-butynylamide)s form a tight helix (dihedral angle at the single bond in the main chain: ca. 70°) surrounded by three hydrogen-bonding strands formed between amide groups at *n*th and $(n + 3)$th units, while poly(*N*-propargylamide)s form a loose helix (dihedral angle at the single bond in the main chain: ca. 130°) surrounded by two hydrogen-bonding strands formed between *n*th and $(n + 2)$th units.[30] Good agreement between the observed and predicted CD spectra based on the time-dependent SCF method supported the appropriateness of the helical conformations. Poly(**3**) having a branched methyl group at the α-carbon atom *o*f the acyl group was highly tolerant to MeOH than poly(**2**) and poly(**3**) having a branched *β*-methyl group, presumably due to the shield effect by the methyl group from MeOH. Poly(**4**) carrying lactone exhibited completely different chiroptical responsiveness to heat from that of the other polymers, possibly due to the participation of the lactone moiety in the hydrogen bonds, which was confirmed by the single-crystal X-ray analysis of the monomer.

Acknowledgment. This research was partly supported by a Grant-in-Aid for Science Research in a Priority Area "Super-Hierarchical Structures (No. 446)" from the Ministry of Education, Culture, Sports, Science, and Technology, Japan. The authors thank Ms. Kayo Terada at Kyoto University for the measurement of the X-ray crystallography data.

References and Notes

(1) (a) Saenger, W. *Principles of Nucleic Acid Structure*; Springer-Verlag: New York, 1984. (b) Watson, J. D.; Crick, F. H. C. *Nature* (*London*) **1953**, *171*, 737−738.

(2) (a) Pauling, L.; Corey, R. B.; Branson, H. R. *Proc. Natl. Acad. Sci. U.S.A.* **1951**, *37*, 205−211. (b) Schulz, G. E.; Schirmer, R. H. *Principles of Protein Structure*; Springer-Verlag: New York, 1979.

(3) Natta, G.; Pino, P.; Corradini, P.; Danusso, F.; Mantica, E.; Nazzanti, G.; Moraglio, G. *J. Am. Chem. Soc.* **1955**, *77*, 1708−1710.

(4) (a) Yamamoto, C.; Okamoto, Y. *Bull. Chem. Soc. Jpn.* **2004**, *77*, 227−257. (b) Habaue, S.; Okamoto, Y. *Chem. Rec.* **2001**, *1*, 46−52. (c) Nakano, T.; Okamoto, Y. *Chem. Rev.* **2001**, *101*, 4013−4038. (d) Okamoto, Y.; Suzuki, K.; Ohta, K.; Hatada, K.; Yuki, H. *J. Am. Chem. Soc.* **1979**, *101*, 4763−4765.

(5) (a) Ute, K.; Hirose, K.; Kashimoto, H.; Hatada, K.; Vogl, O. *J. Am. Chem. Soc.* **1991**, *113*, 6305−6306. (b) Corley, L. S.; Vogl, O. *Polym. Bull.* (*Berlin*) **1980**, *3*, 211−217.

(6) (a) Onitsuka, K.; Mori, T.; Yamamoto, M.; Takei, F.; Takahashi, S. *Macromolecules* **2006**, *39*, 7224−7231. (b) Cornelissen, J. J. L. M.; Graswinckel, W. S.; Rowan, A. E.; Sommerdijk, N. A. J. M.; Nolte, R. J. M. *J. Polym. Sci., Part A: Polym. Chem.* **2003**, *41*, 1725−1736. (c) Cornelissen, J. J. L. M.; Rowan, A. E.; Nolte, R. J. M.; Sommerdijk, N. A. J. M. *Chem. Rev.* **2001**, *101*, 4039−4070. (d) Deming, T. J.; Novak, B. M. *J. Am. Chem. Soc.* **1993**, *115*, 9101−9111.

(7) (a) Muellers, B. T.; Park, J. W.; Brookhart, M. S.; Green, M. M. *Macromolecules* **2001**, *34*, 572−581. (b) Green, M. M.; Park, J.; Sato, T.; Teramoto, A.; Lifson, S.; Selinger, R. L. B.; Selinger, J. V. *Angew. Chem., Int. Ed.* **1999**, *38*, 3139−3154. (c) Green, M. M.; Andreola, C.; Muñoz, B.; Reidy, M. P.; Zero, K. *J. Am. Chem. Soc.* **1988**, *110*, 4063−4065. (d) Goodman, M.; Chen, S. *Macromolecules* **1970**, *4*, 398−402.

(8) (a) Saxena, A.; Rai, R.; Kim, S. Y.; Fujiki, M.; Naito, M.; Okoshi, K.; Kwak, G. *J. Polym. Sci., Part A: Polym. Chem.* **2005**, *44*, 5060−5075. (b) Sato, T.; Terao, K.; Teramoto, A.; Fujiki, M. *Polymer* **2003**, *44*, 5477−5495. (c) Fujiki, M. *J. Am. Chem. Soc.* **1994**, *116*, 6017−6018. (d) Fujiki, M. *J. Am. Chem. Soc.* **1994**, *116*, 11976−11981.

(9) (a) Petit, M.; Daoudi, A.; Ismaili, M.; Buisine, J. M. *Eur. Phys. J. E* **2006**, *20*, 327−333. (b) Reggelin, M.; Schultz, M.; Holbach, M. *Angew. Chem., Int. Ed.* **2002**, *41*, 1614−1617. (c) Muller, C. A.; Hoffart, T.; Holbach, M.; Reggelin, M. *Macromolecules* **2005**, *38*, 5375−5380.

(10) (a) Sedláček, J.; Vohlídal, *J. Collect. Czech. Chem. Commun.* **2003**, *68*, 1745−1790. (b) Tabata, M.; Sone, T.; Sadahiro, Y. *Macromol. Chem. Phys.* **1999**, *200*, 265−282. (c) Kishimoto, Y.; Itou, M.; Miyake, T.; Ikariya, T.; Noyori, R. *Macromolecules* **1995**, *28*, 6662−6666. (d) Furlani, A.; Napoletano, C.; Russo, M. V.; Camus, A.; Marsich, N. *J. Polym. Sci., Part A: Polym. Chem.* **1989**, *27*, 75−86. (e) Furlani, A.; Napoletano, C.; Russo, M. V.; Feast, W. *J. Polym. Bull.* (*Berlin*) **1986**, *16*, 311−317.

(11) (a) Maeda, K.; Mochizuki, H.; Watanabe, M.; Yashima, E. *J. Am. Chem. Soc.* **2006**, *128*, 7639−7650. (b) Otsuka, I.; Sakai, R.; Satoh, T.; Kakuchi, R.; Kaga, H.; Kakuchi, T. *J. Polym. Sci., Part A: Polym. Chem.* **2005**, *43*, 5855−5863. (c) Li, B. S.; Cheuk, K. K. L.; Ling, L. S.; Chen, J. W.; Xiao, X. D.; Bai, C. L.; Tang, B. Z. *Macromolecules* **2003**, *36*, 77−85. (d) Nakako, H.; Nomura, R.; Masuda, T. *Macromolecules* **2001**, *34*, 1496−1502. (e) Nakako, H.; Mayahara, Y.; Nomura, R.; Tabata, M.; Masuda, T. *Macromolecules* **2000**, *33*, 3978−3982. (f) Aoki, T.; Shinohara, K.; Kaneko, T.; Oikawa, E. *Macromolecules* **1996**, *29*, 4192−4198.

(12) (a) Onouchi, H.; Hasegawa, T.; Kashiwagi, D.; Ishiguro, H.; Maeda, K.; Yashima, E. *Macromolecules* **2005**, *38*, 8625−8633. (b) Morino, K.; Oobo, M.; Yashima, E. *Macromolecules* **2005**, *38*, 3461−3468. (c) Kakuchi, R.; Sakai, R.; Otsuka, I.; Satoh, T.; Kaga, H.; Kakuchi, T. *Macromolecules* **2005**, *38*, 9441−9447.

(13) (a) Tabei, J.; Shiotsuki, M.; Sanda, F.; Masuda, T. *Macromolecules* **2005**, *38*, 5860−5867. (b) Tabei, J.; Nomura, R.; Shiotsuki, M.; Sanda, F.; Masuda, T. *Macromol. Chem. Phys.* **2005**, *206*, 323−332. (c) Tabei, J.; Nomura, R.; Sanda, F.; Masuda, T. *Macromolecules* **2004**, *37*, 1175−1179. (d) Tabei, J.; Nomura, R.; Masuda, T. *Macromolecules* **2002**, *35*, 5404−5409. (e) Nomura, R.; Tabei, J.; Masuda, T. *Macromolecules* **2002**, *35*, 2955−2961. (f) Nomura, R.; Tabei, J.; Masuda, T. *J. Am. Chem. Soc.* **2001**, *123*, 8430−8431.

(14) Rodoríguez-Conesa, S.; Candal, P.; Jiménez, C.; Rodríguez, J. *Tetrahedron Lett.* **2001**, *42*, 6699−6702.

(15) Kunishima, M.; Kawachi, C.; Morita, J.; Terao, K.; Iwasaki, F.; Tani, S. *Tetrahedron* **1999**, *55*, 13159−13170.

(16) Halgren, T. A. *J. Comput. Chem.* **1996**, *17*, 490.

(17) (a) Komori, H.; Inai, Y. *J. Phys. Chem. A* **2006**, *110*, 9099. For the ZINDO/S method, see: (b) Zerner, M. C.; Loew, G. H.; Kirchner, R. F.; Mueller-Westerhoff, U. T. *J. Am. Chem. Soc.* **1980**, *102*, 589. (c) Ridley, J. E.; Zerner, M. C. *Theo. Chim. Acta* **1973**, *32*, 111. For the ZINDO-based prediction of CD spectra, see also: (d) Ankai, E.; Sakakibara, K.; Uchida, S.; Uchida, Y.; Yokoyama, Y.; Yokoyama, Y. *Bull. Chem. Soc. Jpn.* **2001**, *74*, 1101. (e) Telfer, S. G.; Tajima, N.; Kuroda, R. *J. Am. Chem. Soc.* **2004**, *126*, 1408.

(18) (a) Frisch, M. J.; Trucks, G. W.; Schlegel, H. B.; Scuseria, G. E.; Robb, M. A.; Cheeseman, J. R.; Montgomery, J. A., Jr.; Vreven, T.; Kudin, K. N.; Burant, J. C.; Millam, J. M.; Iyengar, S. S.; Tomasi, J.; Barone, V.; Mennucci, B.; Cossi, M.; Scalmani, G.; Rega, N.; Petersson, G. A.; Nakatsuji, H.; Hada, M.; Ehara, M.; Toyota, K.; Fukuda, R.; Hasegawa, J.; Ishida, M.; Nakajima, T.; Honda, Y.; Kitao, O.; Nakai, H.; Klene, M.; Li, X.; Knox, J. E.; Hratchian, H. P.; Cross, J. B.; Bakken, V.; Adamo, C.; Jaramillo, J.; Gomperts, R.; Stratmann, R. E.; Yazyev, O.; Austin, A. J.; Cammi, R.; Pomelli, C.; Ochterski, J. W.; Ayala, P. Y.; Morokuma, K.; Voth, G. A.; Salvador, P.; Dannenberg, J. J.; Zakrzewski, V. G.; Dapprich, S.; Daniels, A. D.; Strain, M. C.; Farkas, O.; Malick, D. K.; Rabuck, A. D.; Raghavachari, K.; Foresman, J. B.; Ortiz, J. V.; Cui, Q.; Baboul, A. G.; Clifford, S.; Cioslowski, J.; Stefanov, B. B.; Liu, G.; Liashenko, A.; Piskorz, P.; Komaromi, I.; Martin, R. L.; Fox, D. J.; Keith, T.; Al-Laham, M. A.; Peng, C. Y.; Nanayakkara, A.; Challacombe, M.; Gill, P. M. W.; Johnson, B.; Chen, W.; Wong, M. W.; Gonzalez, C.; Pople, J. A. *Gaussian 03, Revision C.02*; Gaussian, Inc.: Wallingford CT, 2004. For the methods and full references in Gaussian 03, see: (b) The Official Gaussian Website (http://www.gaussian.com).

(19) Harada, N.; Nakanishi, K. Circular Dichroic Spectroscopy. *Exciton Coupling in Organic Stereochemistry*; University Science Books: Mill Valley, CA, 1983.

(20) (a) Maeda, K.; Goto, H.; Yashima, E. *Macromolecules* **2001**, *34*, 1160−1164. (b) Mitsuyama, M.; Ishii, R.; Kondo, K. *J. Polym. Sci., Part A: Polym. Chem.* **2000**, *38*, 3419−3427. (c) Russo, M. V.; Furlani, A.; D'Amote, R. *J. Polym. Chem., Part A: Polym. Chem.* **1998**, *36*, 93−102. (d) D'Amoto, R.; Sone, T.; Tabata, M.; Sadahiro, Y.; Russo, M. V.; Furlani, A. *Macromolecules* **1998**, *31*, 8660−8665.

(21) Calculated by a semiempirical molecular orbital method using the AM1 hamiltonian, Fujitsu MOPAC 2002 Version 2.5.3 on CAChe Version 7.5.

(22) (a) Sanda, F.; Nishiura, S.; Shiotsuki, M.; Masuda, T. *Macromolecules* **2005**, *38*, 3075−3078. (b) Nomura, R.; Nishiura, S.; Tabei, J.; Sanda, F.; Masuda, T. *Macromolecules* **2003**, *36*, 5076−5080.

(23) Percec, V.; Obata, M.; Rudick, J. G.; De, B. B.; Glodde, M.; Bera, T. K.; Magonov, S. N.; Balagurusamy, V. S. K.; Heiney, P. A. *J. Polym. Sci., Part A: Polym. Chem.* **2002**, *40*, 3509−3533.
(24) (a) Nakashima, H.; Koe, J. R.; Torimitsu, K.; Fujiki, M. *J. Am. Chem. Soc.* **2001**, *123*, 4847−4848. (b) Lermo, E. R.; Langeveld-Voss, B. M. W.; Janssen, R. A. J.; Meijer, E. W. *Chem. Commun.* **1999**, 791−792. (c) Ramos, E.; Bosch, J.; Serrano, J. L.; Sierra, T.; Veciana, J. *J. Am. Chem. Soc.* **1996**, *118*, 4703−4704.
(25) The mixtures of **1** with various (*R*)/(*S*)-ratios were prepared from **1** [(*R*)-form] and racemic **1** [1:1 mixture of (*R*)- and (*S*)-forms], which was synthesized from racemic 3-methylpentanoic acid in a manner similar to **1.**
(26) For the molecular graphics, see: Thompson, M. A. ArgusLab 4.0. Planaria Software LLC: Seattle, WA, 2004 (http://www.arguslab.com).
(27) For the terminology of (*P*)- or (*M*)-helix, see: (a) Moss, G. P. *Pure Appl. Chem.* **1996**, *68*, 2193−2222. (b) Cahn, R. S.; Ingold, C. K.; Prelog, V. *Angew. Chem., Int. Ed. Engl.* **1966**, *5*, 385−415.
(28) (a) Furche, F.; Ahlrichs, R.; Wachsmann, C.; Weber, E.; Sobanski, A.; Vögtle, F.; Grimme, S. *J. Am. Chem. Soc.* **2000**, *122*, 1717−1724. (b) Hutchison, G. R.; Ratner, M. A.; Marks, T. J. *J. Phys. Chem. A* **2002**, *106*, 10596−10605.
(29) Tommasini, M.; Zerbi, G.; Chernyak, V.; Mukamel, S. *J. Phys. Chem. A* **2001**, *105*, 7057−7071.
(30) Sanda, F.; Tabei, J.; Shiotsuki, M.; Masuda, T. *Sci. Tech. Adv. Mater.* **2006.** *7*, 572−577.

MA702316F